Published in final edited form as:
J Drug Target. 2007 ; 15(7-8): 538–545. doi:10.1080/10611860701498203.

Enhanced transfection of tumor cells *in vivo* using "Smart" pH-sensitive TAT-modified pegylated liposomes

Amit A. Kale and **Vladimir P. Torchilin**
Department of Pharmaceutical Sciences and Center for Pharmaceutical Biotechnology and Nanomedicine, Northeastern University, 360 Huntington Avenue, Boston, MA 02115, USA

Abstract

Liposomes have been prepared loaded with DNA (plasmid encoding for the green fluorescent protein, GFP) and additionally modified with TATp and PEG, with PEG being attached to the liposome surface via both pH-sensitive hydrazone and non-pH-sensitive bonds. The pGFP-loaded liposomal preparations have been administered intratumorarly in tumor-bearing mice and the efficacy of tumor cell transfection was followed after 72 h. The administration of pGFP–TATp–liposomes with non-pH-sensitive PEG coating has resulted in only minimal transfection of tumor cells because of steric hindrances for the liposome-to-cell interaction created by the PEG coat, which shielded the surface-attached TATp. At the same time, the administration of pGFP–TATp–liposomes with the low pH-detachable PEG resulted in at least three times more efficient transfection since the removal of PEG under the action of the decreased intratumoral pH leads to the exposure of the liposome-attached TATp residues, enhanced penetration of the liposomes inside tumor cells and more effective intracellular delivery of the pGFP. This result can be considered as an important step in the development of tumor-specific stimuli-sensitive drug and gene delivery systems.

Keywords

Pharmaceutical nanocarriers; liposomes; pH-sensitive PEG–PE conjugates; green fluorescent protein; *in vivo* transfection; cancer cells

Introduction

Since the intracellular transport of different biologically active molecules, including DNA, is one of the key problems in drug delivery in general, multiple attempts have been made to bring pharmaceutical nanocarriers, including liposomes and polymeric micelles, directly into the cytoplasm (Weinstein et al. 1979; Weissig et al. 1998; Cryan et al. 2004; Gemeinhart et al. 2005; Oishi et al. 2006; Sawant et al. 2006; Lin et al. 2007). Cell-penetrating (CPPs, such as TAT peptide, TATp) have been successfully used for the intracellular delivery of various small and large molecules and even nanoparticulates (Torchilin et al. 2003b; Albarran et al. 2005; Kleemann et al. 2005; Patel et al. 2006; Renigunta et al. 2006; Sawant et al. 2006). Certainly, to achieve the efficient intracellular delivery of drug-loaded nanocarriers, they have to stay in the blood long enough to provide good accumulation in the pathological area, i.e. be long-circulating. So, it is a tempting idea to have a bifunctional pharmaceutical

Correspondence: V. P. Torchilin, Department of Pharmaceutical Sciences and Center for Pharmaceutical Biotechnology and Nanomedicine, Northeastern University, 312, Mugar Hall, 360, Huntington Avenue, Boston, MA 02115, USA. Tel: 1 617 373 3206. Fax: 1 617 373 8886. v.torchilin@neu.edu.

carrier, which can first accumulate in the required organ or tissue, and then penetrate the cells and bring in its load, including DNA, intracellularly. Initial tissue (tumor) accumulation could be achieved by the passive targeting via the enhanced permeability and retention (EPR) effect (Cabiaux 2004; Sawant et al. 2006), while the subsequent intracellular delivery could be mediated, for example, by CPPs.

Recently, we have described pharmaceutical nanocarriers (liposomes and micelles), which simultaneously carry on their surface both, a cell-penetrating function attached to the surface via a short spacer-arm and sterically- protective polymer (PEG) of higher length than the CPP's spacer and attached to the surface via a pH-sensitive hydrazone bond (Sawant et al. 2006). Such a combination is expected to allow for the longevity of pharmaceutical nanocarriers in the blood and their effective EPR-mediated accumulation in the pathological areas with "leaky" vasculature. During this time, the CPP function should remain hidden, being shielded by extended chains of PEG. However, upon accumulating in a target such as a tumor, where the local interstitial pH value is significantly lower than the normal physiological pH, the protecting polymer should detach because of the hydrolysis of the hydrazone bond under the action of the local lowered pH and expose the previously hidden CPP function mediating the subsequent delivery of the carrier and its cargo inside cells. One would expect such bifunctional carriers to be stable in the blood for few hours for an efficient target accumulation, but to lose PEG coat fast when inside the target tissue to facilitate rapid cellular uptake. The rate of the protective coat elimination can be controlled by the chemical structure of the hydrolizable bond (Kale and Torchilin 2007).

In this study, for the first time we have attempted to test such systems *in vivo*. With this in mind, we have prepared liposomes loaded with DNA (plasmid encoding for the green fluorescent protein, GFP) and additionally modified with TATp and PEG, with PEG being attached to the liposome surface via both pH-sensitive and non-pH-sensitive bonds. These preparations have been administered intratumorally in tumor-bearing mice and the efficacy of tumor cell transfection was followed. One could expect that in the case of non-pH-sensitive PEG coating, the constructs will interact with cells only to a minimal extent because of barrier function of PEG, while in the case of pH-detachable PEG the protective coat should be lost fast inside the tumor, and exposed TATp moieties should allow for effective intracellular penetration of the liposome–DNA complexes and increased transfection outcome.

Materials and methods

Materials

Egg phosphatidylcholine (egg PC), cholesterol (Ch), 1,2-distearoyl-sn-glycero-3-phosphoethanolamine-*N*-[methoxy(polyethylene glycol)-2000] ($mPEG_{2000}$–DSPE), 1,2-dioleoyl-3-trimethylammonium-propane (DOTAP), 1,2-dioleoyl-sn-glycero-3-phosphoethanolamine-*N*-(lissamine rhodamine B sulfonyl) (ammonium salt) (Rh-PE), and phosphatidylthioethanolamine (DPPE-SH) were purchased from Avanti Polar Lipids (Alabaster, AL); mPEG-SH was from Nektar Therapeutics (Huntsville, AL); maleimide-PEG_{1000}–NHS—from Quanta Biodesign (Powell, OH); TATp-cysteine—from Research Genetics (Huntsville, AL). Succinimidyl 4-(*N*-maleimidomethyl)cyclohexane-1-carboxylate hydrazide (SMCCHz) was purchased from Molecular Biosciences (Boulder, CO). 4-Acetyl phenyl maleimide, Sephadex G25m, and Sepharose CL4B were purchased from Sigma-Aldrich. Lewis lung carcinoma (LLC) cell line was purchased from ATCC (Rockville, MD). Delbecco's minimal essential medium, complete serum free medium and fetal bovine serum were purchased from Cellgro (Kansas City, MO).

All synthetic reactions were monitored by TLC using 0.25 mm × 7.5 cm silica plates with UV-indicator (Merck 60F-254), and mobile phase chloroform:methanol (80:20% v/v). Phospholipid and PEG alone or their conjugates were visualized by iodine, phosphomolybdic acid and Dragendorff spray reagents. Silica gel (240–360 μm) and size exclusion media, Sepharose CL4B (40–165 μm) and Sephadex G25m (Sigma-Aldrich), were used for silica column chromatography and size exclusion chromatography, respectively. ^{1}H-NMR spectra were obtained on Varian Unity AS500 instrument (500 MHz). Chemical shifts (δ) were given in ppm relative to TMS.

Methods

Synthesis of aromatic ketone-derived hydrazone-based PEG–PE conjugate

Synthesis of hydrazide derivative PEG: mPEG-SH (MW 2000), **1**, was reacted with 2 M excess of SMCCHz, **2**, in presence of triethylamine for 8 h in dry chloroform. Chloroform was evaporated, and the residue was dissolved in water. The PEG-hydrazide derivative, **3**, was separated and purified by the size exclusion gel chromatography using Sephadex G25m media. The product was freeze-dried and stored as chloroform solution at −80°C. ^{1}H NMR: 1.32–1.35 (t, 1H, 15), 1.79 (s, 1H), 1.87 (m, 2H), 1.99 (s, 1H), 2.16 (s, 1H), 2.46–2.48 (m, 2H), 3.11–3.15 (m, 2H), 3.37 (s, 3H), 3.48–3.50 (m, 2H), 3.53–3.55 (m, 3H), 3.63–3.65 (m, 230H), 3.71–3.72 (m, 2H) and 3.76–3.78 (m, 1H) (Schemes 1–3).

Activation of phospholipid with 4-acetyl phenyl maleimide: Forty micromoles of 4-acetyl phenyl maleimide, **4**, were reacted with 27μmol of phosphatidylthioethanol (DPPE-SH), **5**, in presence of triethylamine overnight with constant stirring under inert atmosphere of argon. The product, **6**, was separated on a silica gel column using chloroform:methanol mobile phase (4:1 v/v). The fractions containing product were identified by TLC analysis, pooled and concentrated. Aromatic ketone-activated phospholipid was stored as chloroform solution at −80°C. ^{1}H NMR: 0.86–0.88 (t, 6H, 20), 1.23–1.24 (m, 55H), 1.51–1.53 (m, 4H), 1.71(s, 18H), 2.17 (s, 1H), 2.21–2.25 (m, 4H), 2.58 (s, 4H), 3.24 (m, 2H), 3.94–4.12 (m, 6H), 7.42–7.43 (m, 1H) and 7.97–7.98 (m, 1H).

Synthesis of mPEG–HZ–PE conjugate: Hydrazide-activated PEG derivative, **3**, was reacted with 1.5 M excess of the aromatic ketone-derivatized phospholipid, **6**, overnight under the constant stirring at room temperature. The PEG–HZ–PE conjugate was separated and purified by size exclusion gel chromatography using Sepharose-CL4B media. ^{1}H NMR: 0.86–0.88 (t, 6H, 20), 1.24 (m, 55H), 1.32–1.34 (t, 1H, 12), 1.63 (m, 65H), 2.17 (s, 3H), 2.18 (s, 1H), 2.25–2.29 (m, 3H), 2.47–2.49 (m, 2H), 3.37 (s, 3H), 3.48–3.50 (m, 5H), 3.53–3.55 (m, 7H), 3.54–3.58 (m, 254H), 7.36–7.38 (m, 1H) and 7.79–7.83 (m, 1H).

Synthesis of PE–PEG$_{1000}$–TATp

Synthesis of PE–PEG$_{1000}$–maleimide: About 1.5 M excess of DOPE-NH$_2$, **8**, was reacted with NHS–PEG$_{1000}$–maleimide, **9**, in chloroform under argon at room temperature in presence of 3 M excess triethylamine overnight with stirring. The product PE–PEG$_{1000}$–maleimide, **10**, was separated on the Sephadex G25m column equilibrated overnight with the degassed double deionized water. The product was freeze-dried and stored under chloroform at −80°C (Scheme 4).

Synthesis of PE–PEG$_{1000}$–TATp: Two-fold molar excess of TATp-SH was mixed with PE–PEG$_{1000}$–maleimide, **10**, in chloroform under inert atmosphere with gentle shaking for 8 h. The excess TATp-SH was separated from the product, **11**, by gel filtration chromatography using Sephadex G25m media. The freeze-dried product was stored under chloroform at −80°C until further use.

***In vitro* pH-dependent degradation of PEG–HZ–PE conjugates:** The time-dependent degradation of mPEG–HZ–PE (micelles) in buffer solutions of different pHs at 37°C was followed by HPLC using the Shodex KW-804 size exclusion column (Sawant et al. 2006; Kale and Torchilin 2007). In brief, the elution buffer used was pH 7.0, phosphate buffer (100 mM phosphate, 150 mM sodium sulfate), run at 1.0 ml/min. For the fluorescent detection of the micelle peak, Rh-PE (1% mol of mPEG–PE; Ex 550 nm/Em 590 nm) was added to the mPEG–PE conjugate in chloroform. A film was prepared by evaporating the chloroform under argon stream and then hydrated with the phosphate buffer saline pH 7.4, 7, 6.5, 6.0, 5.5 or 5.0 (adjusted with 0.1 N HCl). A peak that represents the micelle population appeared at the retention time between 9 and 10 min. The degradation kinetics of micelles was assessed by following the area under the micelle curve.

Preparation of the liposomal formulations: The pH-sensitive or pH-insensitive, TATp-bearing pGFP-complexed liposomes were prepared by the spontaneous vesicle formation (SVF) method adopted from (Jeffs et al. 2005) with few modifications. A plasmid solution was prepared by combining pGFP and 10 mM Tris–EDTA (TE) buffer, pH 7.4. A lipid solution in ethanol was prepared by dissolving egg PC:Chol (7:3) in anhydrous ethanol, and then adding DOTAP, TATp–PEG_{1000}–PE and either $mPEG_{2000}$–HZ–PE (**7**, pH-sensitive) or $mPEG_{2000}$–DSPE (pH-insensitive) at 10:0.25:15 M ratio. The charge (±) ratio was 10:1. The lipid and plasmid solutions were preheated to 37°C before mixing together. After mixing these solutions for 10 min, ethanol was evaporated under the reduced pressure. The samples were filtered through 0.2 μm polycarbonate filters and stored at 4°C until use. The liposomal formulations were subjected to the agarose gel electrophoresis to test for the quantitative presence and intactness of the plasmid within the liposomes (Torchilin et al. 2003a). In a typical case, the pGFP concentration was 3.22 μg/mg of total lipid. The liposome particle mean size and size distribution were observed using a Coulter N4 Plus submicron particle analyzer.

***In vivo* transfection with pGFP:** LLC tumors were grown in nu/nu mice (Charles River Breeding Laboratories, MA) by the s.c. injection of 8×10^4 LLC cells per mouse into the left flank (protocol # 05-1233R, approved by the Institutional Animal Care and Use Committee at Northeastern University, Boston). When tumor reached 5–10 mm in diameter, they were injected at four to five different spots with 150 μl of pGFP-loaded, TATp-bearing pH-sensitive or pH-insensitive liposomes in phosphate-buffered saline, pH 7.4. Mice were killed 72 h later by cervical dislocation, and excised tumors were fixed in a 4% buffered paraformaldehyde overnight at 4°C, blotted dry of excess paraformaldehyde and kept in 20% sucrose in PBS overnight at 4°C. Cryofixation was done by the immersion of tissues in ice-cold isopentane for 3 min followed by freezing at −80°C. Fixed, frozen tumors were mounted in Tissue-Tek OCT 4583 compound (Sakura Finetek, Torrance, CA) and sectioned on a Microtome Plus (TBS). Sections were mounted on slides and analyzed by the fluorescence microscopy using FITC filter and with hematoxylin –eosin staining. The images were analyzed using ImageJ 1.34I software (NIH) for integrated density comparison of green fluorescence between pH-sensitive and pH-insensitive groups.

Results and discussion

Synthesis of pH-sensitive PEG–PE conjugates

Earlier, we have investigated the *in vitro* hydrolytic degradation kinetics of aliphatic and aromatic aldehyde-derived hydrazone-based PEG–PE conjugates (Kale and Torchlin 2007). We found that aliphatic aldehyde-derived hydrazone-based PEG–PE conjugates were unstable at acidic pH while showed $t_{1/2}$ ranging from 2.5 h to 20 min at pH 7.4 depending on acyl hydrazide used. The PEG–HZ–PE conjugates derived from aromatic aldehydes were

found to be too stable to use as pH-sensitive carriers for targeting. For the particular set of experiments described in this paper, we focused on aromatic ketone-derived hydrazone-based PEG–PE conjugates to tune the hydrolytic degradation kinetics in such a way that the conjugates would be sufficiently stable at physiological pH (~ half-life of the liposomal carriers, i.e. more stable than aldehyde-derived hydrazones) and degrade fast at mildly acidic pH.

Aromatic ketone-derived hydrazone bond was introduced between PEG and PE via the Schemes 1–3. To synthesize aromatic ketone-derived hydrazone-based mPEG–HZ–PE conjugate, a hydrazide derivative of PEG was prepared by reacting mPEG–SH with SMCCHz in presence of triethylamine. A phospholipid, DPPE-SH, was activated using 4-acetyl phenyl maleimide via the Michael addition at maleimide ring. The aromatic ketone-activated phopsholipid was then reacted with hydrazide derivative of PEG. The identity of conjugates was confirmed by ^{1}HNMR and TLC.

In vitro pH-dependent degradation of PEG–HZ–PE conjugates

Aromatic ketone-derived hydrazone bond was introduced between PEG and PE. The presence of a methyl group (electron donating) on the carbonyl functional group would provide a sufficient lability of the hydrazone bond under mildly acidic conditions while an immediate aromatic ring (electron withdrawing) next to the hydrazone bond would offer the stability under acidic and neutral conditions. mPEG–HZ–PE conjugate, wherein the hydrazone bond is derived from an aromatic ketone, exhibited the half-lives of 2–3 h at slightly acidic pH values, and much higher stability (up to 40 h) at the physiological pH (Table I).

Synthesis of PE–PEG$_{1000}$–TATp conjugate

TATp-SH was attached to the heterobifunctional PEG via the two step synthesis as shown in the Scheme 4. First, Mal–PEG–PE conjugate was synthesized by reacting DOPE–NH_2 with the NHS end of heterobifunctional PEG derivative, **8**, NHS–PEG$_{1000}$–maleimide. PE–PEG$_{1000}$–maleimide was then reacted with TATp-SH to form PE–PEG$_{1000}$–TATp conjugate. The conjugate was separated by gel chromatography using the Sephadex G25m media.

Liposomal formulations

Agarose gel electrophoresis indicated the complete complexation of the plasmid DNA with the liposomal formulations. The mean liposome size was 180 ± 35 nm (polydispersity index 0.24) as monitored by Coulter N4 Plus submicron particle analyzer.

In vivo pGFP transfection experiment

We attempted a localized transfection of tumor cells by the direct intratumoral administration of sterically shielded with pH-sensitive (containing mPEG–HZ–PE, **7**) or pH-insensitive (containing mPEG–DSPE) conjugates TATp–liposome–pGFP complexes into the tumor tissue by the intratumoral injections.

Histologically, hematoxylin/eosin-stained tumor slices in animals injected with both preparations showed the identical typical pattern of poorly differentiated carcinoma (polymorphic cells with basophilic nuclei forming nests and sheets and containing multiple sites of neoangiogenesis; Figure 1(a),(b)). However, under the fluorescence microscope with FITC filter, samples prepared 72 h post-injection from tumors injected with pH-sensitive PEG–TATp–liposome–pGFP complexes demonstrated intensive and bright green fluorescence compared to only minimal GFP fluorescence observed in the samples obtained

from the tumors injected with pH-insensitive PEG–TATp–liposome–pGFP complexes (Figure 2(a),(b)). The ImageJ analysis indicated a three times less effective transfection in the case of PEG–TATp–pGFP-pH-insensitive liposomes as non-detachable PEG coat interferes and sterically hinders the interactions between TATp and target cancer cells (compare (a) and (b) in Figure 2).

The enhanced pGFP transfection by using pH-sensitive PEG–TATp–liposome–pGFP complexes seems to be an ultimate result of the removal of mPEG–HZ–PE coat under the decreased pH of the tumor tissue, and better accessibility of de-shielded TATp moieties in TATp–liposome–pGFP complexes for internalization by the cancer cells allowing for the increased interactions of pGFP with cancer cell nuclei.

Owing to their physicochemical properties, the long-circulating (PEGylated) liposomal carriers have the ability to accumulate inside the tumor tissue via the EPR effect, without further escape into undesired non-target sites. The pH at tumor sites is “acidic” (Engin et al. 1995; Ojugo et al. 1999). Therefore, when TATp–pGFP–liposomes with an additional pH-sensitive PEG coating accumulate in the tumor tissue, the lowered pH-mediated removal of the protective PEG coat takes place, and TATp moieties become exposed and accessible for the interaction with cells. This leads to rapid pGFP pay-load delivery into the cancer cells as result of the extensive TATp-mediated internalization of liposomes, and thereby enhanced transfection.

Conclusion

Thus, intratumorally administered liposomes loaded with DNA and additionally modified with TATp and PEG, with PEG being attached to the liposomes surface via pH-sensitive hydrazone bond, allow for the highly efficient transfection of tumor cells due to the removal of the PEG coat under the action of the decreased intratumoral pH which leads to the exposure of the liposome-attached TATp residues, enhanced penetration of the liposomes inside tumor cells and more effective intracellular delivery of the pGFP. This result can be considered as an important step in the development of tumor-specific stimuli-sensitive drug and gene delivery systems. As the next step, we plan to investigate if the systemic administration of such preparation loaded with anti-cancer drugs or DNA will allow first for their accumulation in tumor via EPR effect and then, already inside tumors, the loss of protective PEG coat will lead to the effective intracellular penetration mediated by the exposed TATp moieties, and enhanced transfection or drug action.

Acknowledgments

This work was supported by the NIH grants RO1 HL55519 and RO1 CA121838 to Vladimir P. Torchilin. Authors thank Drs. Paresh Salgaonkar and Vidyanand Shukla for technical assistance in ^{1}H NMR studies.

References

Albarran B, To R, Stayton PS. A TAT-streptavidin fusion protein directs uptake of biotinylated cargo into mammalian cells. Protein Eng Des Sel. 2005; 18(3):147–152. [PubMed: 15820981]

Cabiaux V. pH-sensitive toxins: Interactions with membrane bilayers and application to drug delivery. Adv Drug Deliv Rev. 2004; 56(7):987–997. [PubMed: 15066756]

Cryan SA, Holohan A, Donohue R, Darcy R, O’Driscoll CM. Cell transfection with polycationic cyclodexrin vectors. Eur J Pharm Sci. 2004; 21(5):625–633. [PubMed: 15066663]

Engin K, Leeper DB, Cater JR, Thistlethwaite AJ, Tupchong L, McFarlane JD. Extracellular pH distribution in human tumours. Int J Hyperthermia. 1995; 11(2):211–216. [PubMed: 7790735]

Gemeinhart RA, Luo D, Saltzman WM. Cellular fate of a modular DNA delivery system mediated by silica nanoparticles. Biotechnol Prog. 2005; 21(2):532–537. [PubMed: 15801794]

Jeffs LB, Palmer LR, Ambegia EG, Giesbrecht C, Ewanick S, MacLachlan I. A scalable, extrusion-free method for efficient liposomal encapsulation of plasmid DNA. Pharm Res. 2005; 22(3):362–372. [PubMed: 15835741]

Kale AA, Torchilin VP. Design, synthesis and charecterization of pH-sensitive PEG–PE conjugates for stimuli-sensitive pharmaceutical nanocarriers: The effect of substitutes at the hydrazone linkage on the pH stability of PEG–PE conjugates. Bioconjug Chem. 2007 (in press).

Kleemann E, Neu M, Jekel N, Fink L, Schmehl T, Gessler T, Seeger W, Kissel T. Nano-carriers for DNA delivery to the lung based upon a TAT-derived peptide covalently coupled to PEG–PEI. J Control Release. 2005; 109(1–3):299–316. [PubMed: 16298009]

Lin C, Zhong Z, Lok MC, Jiang X, Hennink WE, Feijen J, Engbersen JF. Novel bioreducible poly(amido amine)s for highly efficient gene delivery. Bioconjug Chem. 2007; 18(1):138–145. [PubMed: 17226966]

Oishi M, Kataoka K, Nagasaki Y. pH-responsive three-layered PEGylated polyplex micelle based on a lactosylated ABC triblock copolymer as a targetable and endosome-disruptive nonviral gene vector. Bioconjug Chem. 2006; 17(3):677–688. [PubMed: 16704205]

Ojugo AS, McSheehy PM, McIntyre DJ, McCoy C, Stubbs M, Leach MO, Judson IR, Griffiths JR. Measurement of the extracellular pH of solid tumours in mice by magnetic resonance spectroscopy: A comparison of exogenous (19)F and (31)P probes. NMR Biomed. 1999; 12(8): 495–504. [PubMed: 10668042]

Patel J, Galey D, Jones J, Ray P, Woodward JG, Nath A, Mumper RJ. HIV-1 tatcoated nanoparticles result in enhanced humoral immune responses and neutralizing antibodies compared to alum adjuvant. Vaccine. 2006; 24(17):3564–3573. [PubMed: 16516358]

Renigunta A, Krasteva G, Konig P, Rose F, Klepetko W, Grimminger F, Seeger W, Hanze J. DNA transfer into human lung cells is improved with Tat-RGD peptide by caveolimediated endocytosis. Bioconjug Chem. 2006; 17(2):327–334. [PubMed: 16536462]

Sawant RM, Hurley JP, Salmaso S, Kale AA, Tolcheva E, Levchenko T, Torchilin VP. “Smart” drug delivery systems: Double-targeted pH-responsive pharmaceutical nano-carriers. Bioconjug Chem. 2006; 17:943–949. [PubMed: 16848401]

Torchilin VP, Levchenko TS, Rammohan R, Volodina N, Papahadjopoulos-Sternberg B, D’Souza Gerard GM. Cell transfection *in vitro* and *in vivo* with non-toxic TAT petide–liposome–DNA complexes. Proc Natl Acad Sci USA. 2003a; 100(4):1972–1977. [PubMed: 12571356]

Torchilin VP, Levchenko TS, Rammohan R, Volodina N, Papahadjopoulos-Sterberg B, D’Souza GGM. Cell transfection *in vitro* and *in vivo* with non-toxic TAT peptide–liposome–DNA complexes. Proc Natl Acad Sci USA. 2003b; 100(4):1972–1977. [PubMed: 12571356]

Weinstein JN, Magin RL, Yatvin MB, Zaharko DS. Liposomes and local hyperthermia: Selective delivery of methotrexate to heated tumors. Science. 1979; 204(4389):188–191. [PubMed: 432641]

Weissig V, Whiteman KR, Torchilin VP. Accumulation of protein-loaded long-circulating micelles and liposomes in subcutaneous Lewis lung carcinoma in mice. Pharm Res. 1998; 15(10):1552–1556. [PubMed: 9794497]

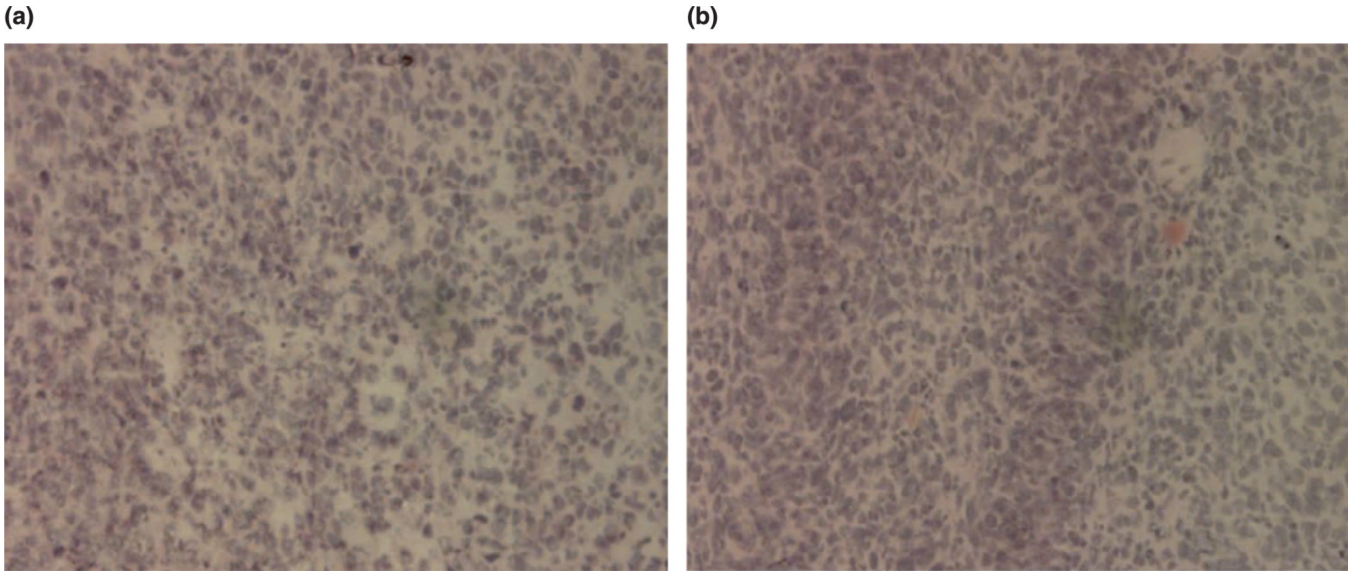

Figure 1.
Histology of tumor tissue after the hematoxylin/eosin staining under bright-field light microscopy. (a) Untreated tumor and (b) treated tumor.

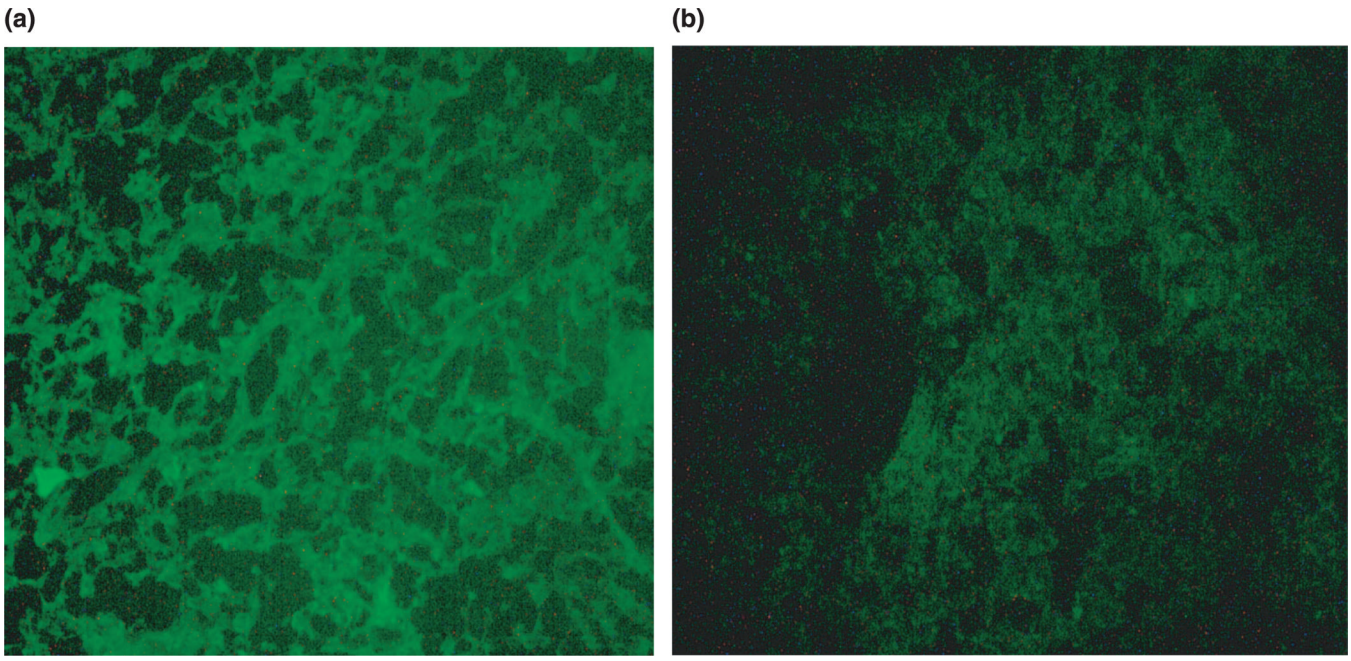

Figure 2.
(a) Fluorescence microscopy images of the LLC tumor sections from the tumors injected with pGFP-loaded TATp-bearing liposomes with the pH-cleavable PEG coat and (b) with the pH-non-cleavable PEG coat.

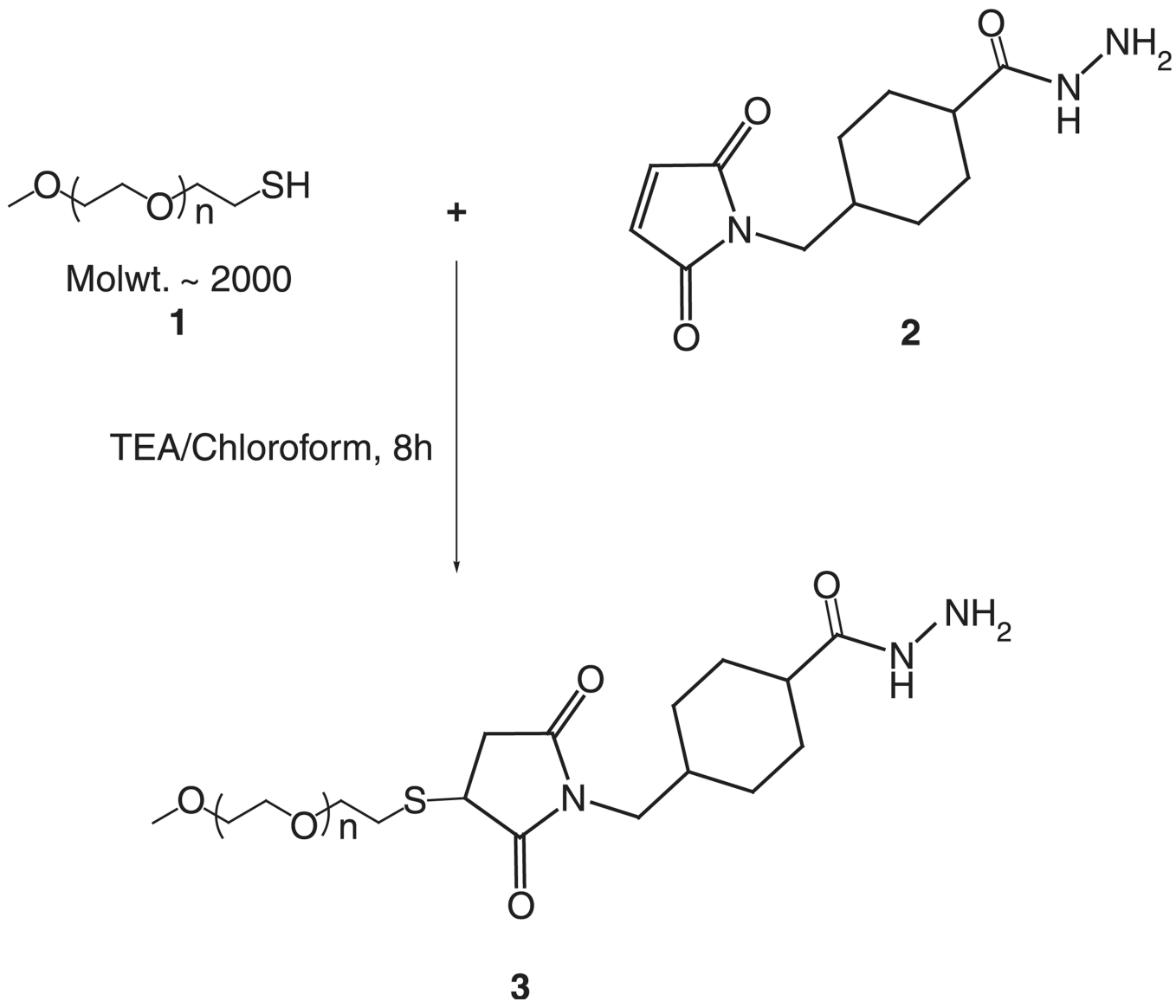

Scheme 1.
Synthesis of hydrazide-activated mPEG.

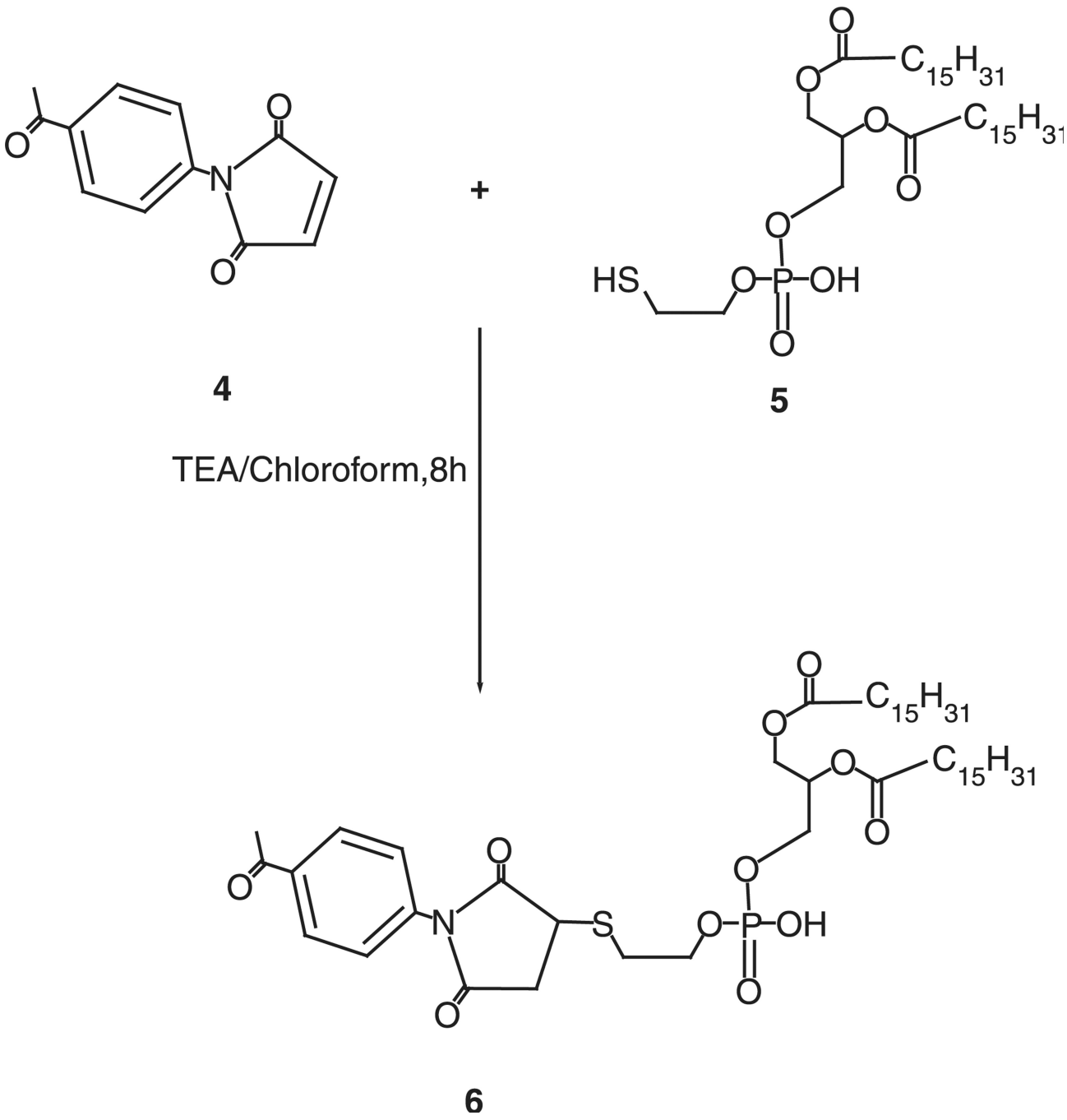

Scheme 2.
Synthesis of aromatic ketone derivative of the phospholipid.

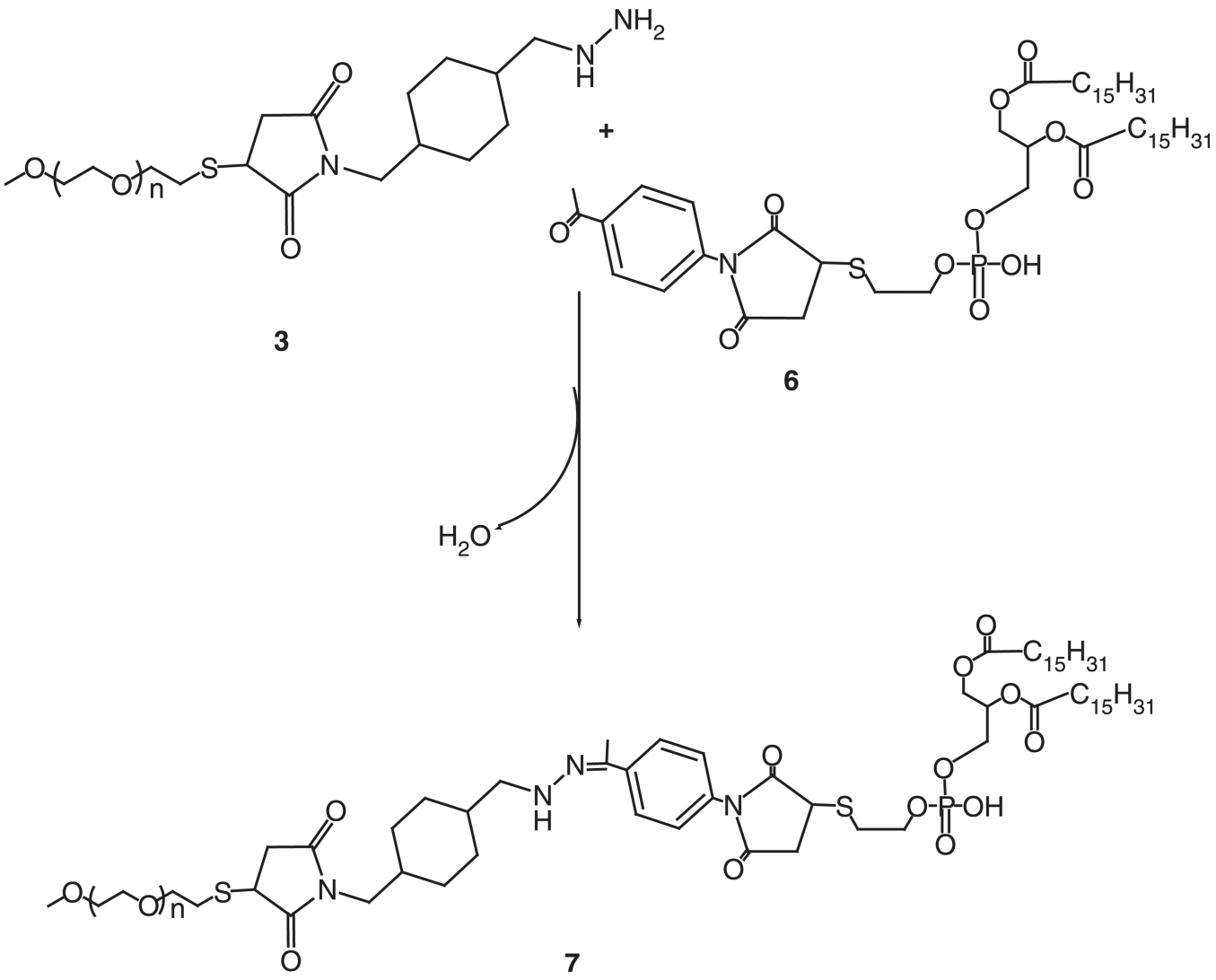

Scheme 3.
Synthesis of aromatic ketone-derived mPEG–HZ–PE conjugate.

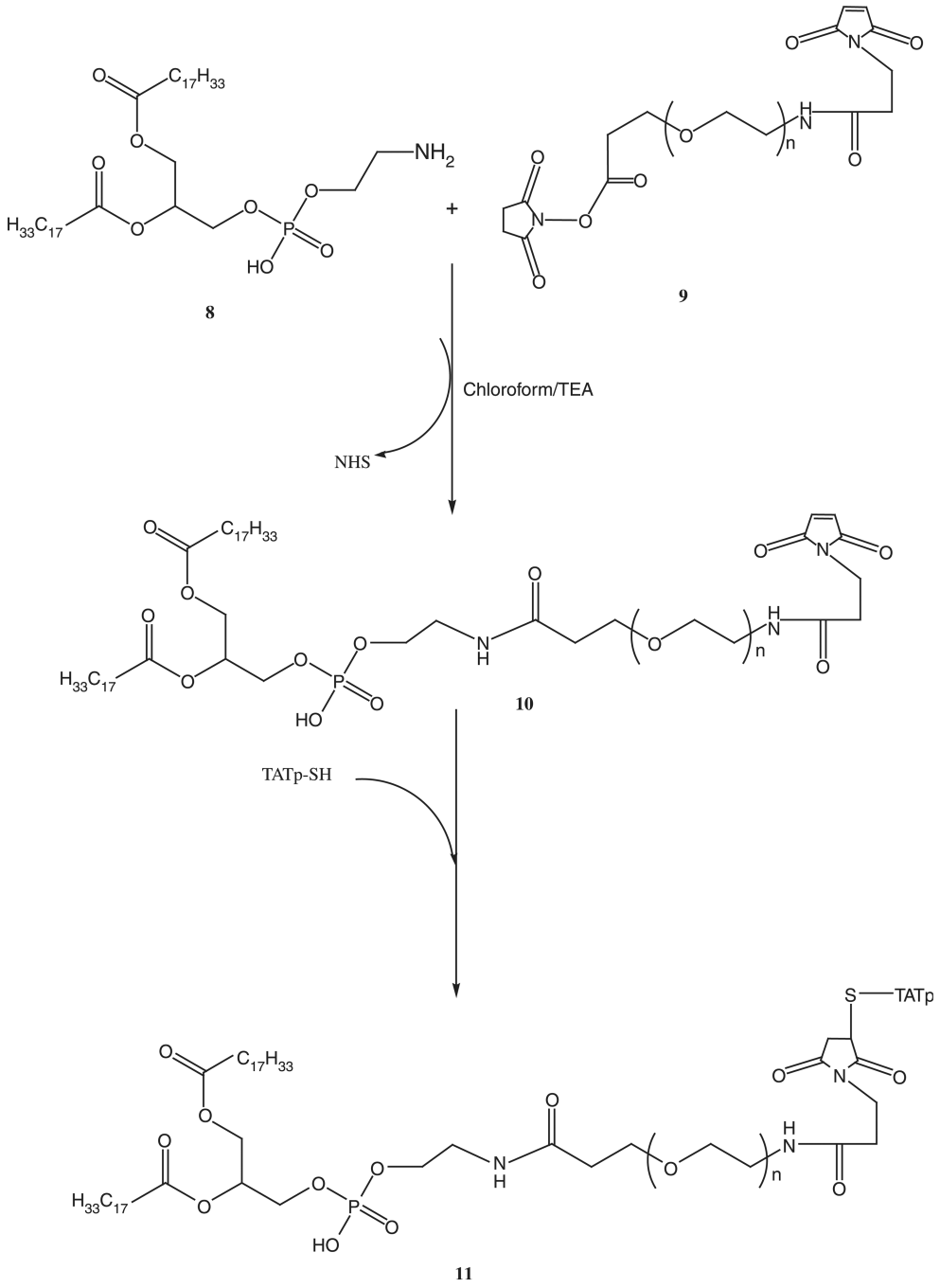

Scheme 4.
Synthesis of PE–PEG$_{1000}$–TATp conjugate.

Table I

pH-dependent hydrolytic kinetics of aromatic ketone-derived (**7**) mPEG–HZ–PE conjugates incubated in different pH buffer solutions at 37°C.

Conjugate	pH	Half-life (h)
MPEG–HZ–PE(7)	7.4	40
	7.0	24
	6.5	12
	6.0	6
	5.5	3
	5.0	2